

# Investigation of Solar-Driven Hydroxy gas production system performance integrated with photovoltaic panels with single-axis tracking system

Farhad Salek<sup>1</sup>, Mohammad Rahnama<sup>1</sup>, Hossein Eshghi<sup>1</sup>, Meisam Babaie<sup>2</sup> and Mohammad Mahdi Naserian<sup>3\*</sup>

1. Faculty of Mechanical and Mechatronic Engineering, Shahrood University of Technology, Shahrood, Iran.

2. School of Computing, Science and Engineering, University of Salford, Manchester, UK.

3. Department of Mechanical Engineering, Faculty of Montazeri, Khorasan Razavi Branch, Technical and Vocational University, Mashhad, Iran.

Receive Date 26 April 2021; Revised Date 08 May 2021; Accepted Date 13 May 2021

\*Corresponding author: m.m.naserian@pgs.usb.ac.ir (M.M. Naserian)

## Abstract

In this work, a solar-driven alkaline electrolyzer producer of hydroxy gas is proposed, which is integrated with photovoltaic panels with a single-axis north-south solar tracking system. The main novelty of this work is providing a transient analysis of integration of an alkaline electrolyzer to the PV panels equipped with a solar tracking system. Furthermore, the transient model of the alkaline electrolyzer is employed in order to calculate its operating temperature, hydroxy production rate, and the other operational parameters at various hours of the day. The electrolyzer and the PV panels with a tracking system are modelled by the EES software. It is assumed that the system is installed in the city of Shahrood, and therefore, the geographical data for this city is used for a seasonal analysis. The effective areas of the electrolyzer electrodes and the PV panels are also assumed to be fixed at 0.25 m<sup>2</sup> and 50 m<sup>2</sup>, respectively, in this work. Based on the results obtained, employment of the solar tracking system results in a significant increment of the PV panel power absorption rate, resulting in a power increment up to 4.2 kW in the summer. On the other hand, the transient analysis of the proposed alkaline electrolyzer shows that the maximum operating temperature reaches 80 °C at around 12 AM in the summer, causing achievement of a maximum electrical current peak in the summer. Therefore, an efficient cooling system should be employed in the summer for the decrement of the alkaline electrolyzer temperature. The proposed system is capable of producing 7.6 m<sup>3</sup>/day, 10.4 m<sup>3</sup>/day, 7.2 m<sup>3</sup>/day, and 4.1 m<sup>3</sup>/day of hydroxy gas in the spring, summer, fall, and winter, respectively.

**Keywords:** Alkaline electrolyzer, hydroxy gas, photovoltaic panel, solar tracker.

## 1. Introduction

Due to the environmental concerns of fossil fuel consumptions across the world, most of the countries are looking for alternative energy resources [1, 2]. One of the most promising fuels for the future is hydrogen gas [3, 4]. Its high flammability and vast applications have made this fuel a reasonable choice to be substituted by the fossil fuels [5]. Water electrolysis [6, 7] and natural gas reforming [8] are two major methods for extracting hydrogen gas. In the reforming method, a catalyst is required to break the chemical bonds in natural gas [9]. Carbon dioxide is a side-product of the foregoing reaction, which can be used in the other processes or is discharged to the environment, which will also cause contamination [8]. Moreover, hydrogen production using the reforming method requires significant resources of natural gas, which are not

accessible all around the world [10-12]. Meanwhile, the water electrolysis method does not require consumption of fossil fuels for production of hydrogen [13, 14]. In this method, only electricity and water are required for the generation of hydrogen [15, 16].

Consequently, this method is considered as one of the sustainable methods for the production of hydrogen [17]. Moreover, it can be coupled to the photovoltaic panels, which generates electricity from solar irradiations in order to provide a stand-alone system [18-20].

There are many types of electrolyzers by which hydrogen can be generated using electrical power such as alkaline electrolyzers (AELs) and proton exchange membrane electrolyzers (PEMELs) [21-23]. AELs are the conventional type used for a sustainable hydrogen production in various

countries [24]. PEMELs have recently achieved attention, and the researchers are working on developing it as a high performance electrolyzer with a higher power density compared to AELs [24]. However, PEMELs are too costly compared to AELs. Therefore, PEMELs are not yet economical to be used in different industries. Furthermore, the structure of AELs is simpler than that of PEMELs (3). A comparison of the alkaline and proton exchange membrane electrolyzers is provided in Table 1.

**Table 1. Alkaline and proton exchange membrane electrolyzer characteristics [25].**

Name	Unit	Alkaline electrolyzer	PEM electrolyzer
Electrolyte	-	KOH or NOH solution	Solid polymer
Current density	A/m <sup>2</sup>	2000-4000	10000-20000
Working pressure	MPa	< 3.2MPa	< 5MPa
Operating temperature	°C	80-90	50-80
Corrosion	-	Alkaline corrosion	No
Manufacturing cost	-	Low	High
Lifetime	years	10	3-4

Therefore, one of the easiest ways for production of pure hydrogen, is the employment of AELs [26, 27]. The employment of this method for production of hydrogen in medium- and small-scales is more economical than the other methods [28]. Potassium hydroxide with concentrations of 25% to 30% is often used in AELs as the electrolyte. One of the major problems of this types of electrolyzers is the high corrosiveness of the electrolyte. When the working temperature rises, the electrode life decreases. Therefore, the working temperature of AELs should be controlled.

The integration of AELs, which produces pure hydrogen with photovoltaic panels, has been studied by many researchers. Fereidooni *et al.* [29] have studied the coupling of the hydrogen production cells with the photovoltaic panels with a constant tilt angle. For the simulation of the system, the characteristics of 20 kW photovoltaic panels, which were installed in Yazd, were used. The energy efficiency of photovoltaic panels was reported as 12.32%, and the hydrogen production rate was estimated to be approximately 373 tons annually. Menad *et al.* [19] have worked on the integration of photovoltaic panels with AELs by considering the climate of a city located in the south of Algeria. In this study, different strategies for controlling the output current of photovoltaic

panels and their effects on the hydrogen extraction have been investigated. According to their reports, using the REF542plus relay in the controlling unit of the system led to an increase in the safety and production efficiency. In another research work, Schnuelle [30] has presented the simulation results for two specific types of electrolyzers including AELs and PEMELs in both the wind and PV power input for the climate of NW Germany. He concluded that the shape of the input power signals and the coupling of the electrolyzers with the other parts of the system had a great impact on the electricity utilization, net production cost, and hydrogen production efficiency. Furthermore, he reported that the AEL technology with a renewable electricity supply was more cost-effective in comparison with the other studied types of electrolyzers. A stand-alone solar-driven hydrogen production system has been designed and studied by Bhattacharyya *et al.* [31], in which the electrolyzers are powered by photovoltaic panels. The PV panels without solar tracking system was modelled mathematically, and the empirical equations were used for prediction of the AEL hydrogen production rate in this study. Based on their results, it was predicted that nearly 60 kW electrical power was required by the PV panels for production of 10 Nm<sup>3</sup>/h of hydrogen. In a another study, the experimental characterization and size optimization of a photovoltaic-driven hydrogen generation system has been studied by Ferrari *et al.* [32]. The results of their work indicated that the hydrogen production efficiency was highly related to the solar irradiation in the location where the photovoltaic panels were installed. Using a finite-time thermo-economic analysis, an optimized economic model was developed in this research work. In a separate study conducted by Cilogullari *et al.* [33] about coupling of photovoltaic thermal (PVT) panels with PEMELs, it was reported that using the PVT panels in system could result in an increase in the hydrogen production performance as well as the photovoltaic efficiency.

It can be seen from the literature that different researchers have focused on using AELs in order to produce pure hydrogen. Apart from AELs, in which a semi-permeable membrane is used for the production of pure hydrogen, there is another type of AEL that produces a mixture of hydrogen and oxygen gas called hydroxy gas [3, 5]. This type of gas can be used in a combustion process such as in boilers and internal combustion engines for the production of heat and mechanical power, while producing lesser emissions compared to the fossil fuels. On the other hand, the employment of PV

panels with solar tracking systems in solar-driven alkaline hydrogen production systems is still missing. The solar trackers are widely used for increasing the performance and rate of the solar energy absorption of photovoltaic panels [34, 35]. There are many types of solar trackers available such as the multi-axis and single-axis ones. The single-axis north-south solar trackers are capable of changing the tilt angle of the panel for achieving the optimum tilt angle at which the maximum rate of solar energy can be achieved by the PV panels. The main contribution of this study is the time-dependent thermodynamic analysis of the alkaline electrolyzers integrated with PV panels equipped with solar tracking system in order to obtain variations in the electrolyzer functional parameters during the hours of the day. In the current work, the integration of PV panels equipped with single-axis solar trackers with AEL producer of the hydroxy gas is studied in order to provide a stand-alone green fuel production system for remote areas. The AEL and PV panels with solar tracking system is mathematically

modelled using the EES software, and a parametric analysis is performed to obtain the integrated system functional parameter variations in various seasons during the year.

## 2. System description

The proposed system consists of PV panels and AEL components, as it can be seen in Figure 1. The electrical energy produced by the PV panels (equipped with a solar tracker) is transferred to AELs for production of the hydroxy gas. Furthermore, the voltage of electricity flow transferred to AELs is changed by employment of a DC/DC converter (Figure 1). Moreover, by feeding water into AELs, the electrical energy produced by the solar panels is used for water electrolysis, resulting in the production of the hydrogen and oxygen gases, a mixture of which is called hydroxy. The produced hydroxy gas can then be transferred to the boilers or stationary engines, leading to the improvement of their performance and reduction in the emission production.

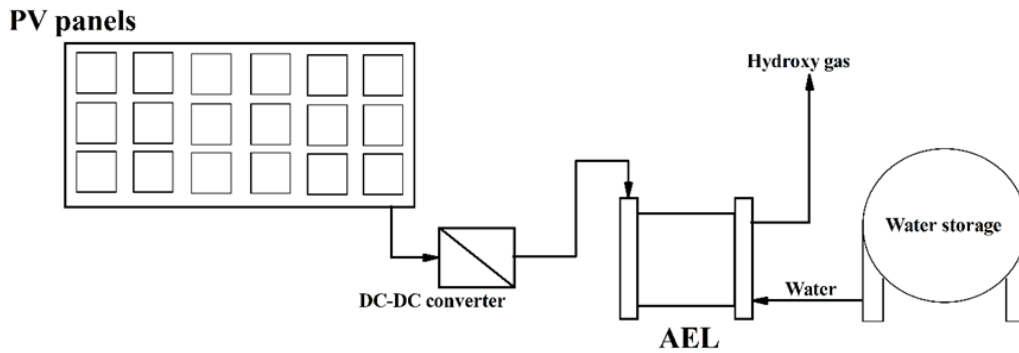


Figure 1. A block diagram of the proposed system.

## 3. Mathematical modelling

### 3.1. PV panels

This system comprises some sub-systems including photovoltaic panels with a north-south solar tracker. The total receiving irradiation for a horizontal plane outside the atmosphere can be calculated by [36, 37]:

$$I_{on} = \frac{43200}{\pi} G_{sc} (1 + 0.033 \cos \frac{360n}{365}) \times [\cos \phi \cos \delta (\sin \omega_2 - \sin \omega_1) + \frac{\pi(\omega_2 - \omega_1)}{180} \sin \phi \sin \delta] \quad (1)$$

where  $\omega_1$  and  $\omega_2$  are the beginning and the end of time interval and are equal to 1 h in the calculations. In addition,  $\phi$  and  $\delta$  are the latitude and axial tilt of the panel, respectively. In order to calculate the amount of hourly solar irradiation on

a tilted plane, the following equations are used [36, 38]:

$$I_o = I_{on} \cos \theta \quad (2)$$

$$\cos \theta = \sin \phi \sin \delta \cos \beta - \cos \phi \sin \delta \sin \beta + \cos \phi \cos \delta \cos \beta \cos \omega + \cos \delta \sin \beta \sin \delta \sin \omega \quad (3)$$

$\beta$  expresses the plane tilt angle. Furthermore, the plane azimuth angle ( $\gamma$ ) was considered to be equal to zero in this work. In order to calculate the total irradiation on a titled plane, the following expression is used [36]:

$$I_T = I_b r_b + I_d \frac{1 + \cos \beta}{2} + I_p \frac{1 - \cos \beta}{2} \quad (4)$$

In the foregoing equation,  $I_b$  and  $I_d$  are the beam and diffused solar irradiances, respectively. In addition,  $r_b$  is the ratio of solar irradiation on the tilted plane horizontal plane. For estimation of the incident angle of the panel with north-south

solar tracking system during the day, the following equation is used [36]:

$$\cos \theta_T = \sin^2 \delta + \cos^2 \delta \cos \omega \quad (5)$$

and the panel tilt angle should be fixed at:

$$\beta_T = |\phi - \delta| \quad (6)$$

Therefore, the solar azimuth angle in this work was calculated from the following equations [36]:

$$\gamma_T = \begin{cases} 0^\circ & \text{if } |\gamma_s| < 90 \\ 180^\circ & \text{if } |\gamma_s| \geq 90 \end{cases} \quad (7)$$

As the efficiency of the photovoltaic panels depends on its cell's temperature, the following equation is used in order to calculate the temperature of the panel surface in this work [39]:

$$T_{PV} = T_{amb} + \left( \frac{T_{NOCT} - 20}{800} \right) \left( \frac{I_T}{3600} \right) \quad (8)$$

where  $T_{amb}$  and  $T_{NOCT}$  are the ambient temperature and normal working temperature, respectively. Moreover,  $T_{NOCT}$  equals to 44 °C, as presented in the literature [39]. After calculation of the temperature of the panel surface, the panel efficiency can be obtained by employment of an equation provided below [39, 40]:

$$\eta_{PV} = \eta_{ref} (1 - \beta_{ref} (T_{PV} - T_{ref})) \quad (9)$$

where  $\eta_{ref}$ ,  $\beta_{ref}$ , and  $T_{ref}$  are considered as 12%, 0.0045, and 25 °C, respectively, in this work [39, 40].

The electrical voltage at the output of DC-DC converter equals to 52 V, and the electrical efficiency of the converter is assumed to be up to 98%. The fill factor for the proposed PV panel equals to 0.69 when the PV cell temperature reaches 40 °C [40].

### 3.2. Alkaline electrolyzer

For simulation of the alkaline electrolyzer, the following assumptions were made in this work [41, 42]:

- Oxygen and hydrogen are ideal gases;
- Water is a compressible liquid;
- The liquid and gas phases are not mixed.

The variations in the Gibbs free energy can be expressed as [41]:

$$\Delta G = \Delta H - T \Delta S \quad (10)$$

where  $\Delta H$  and  $\Delta S$  are the enthalpy and entropy changes during the water splitting process, respectively. The reversible cell voltage that indicates how much electrical energy is required for splitting of water is provided as [41, 42]:

$$V_{rev} = \frac{\Delta G}{zF} \quad (11)$$

where  $z$  and  $F$  are the number of electrons transferred in a reaction (=2 for hydrogen) and Faraday constant (=96485 C/mol), respectively. In addition, the thermo-neutral cell voltage that affects the total energy demand for splitting of water is calculated by [41, 42]:

$$V_{rev} = \frac{\Delta G}{zF} \quad (12)$$

The I-V curve form as the function of temperature for alkaline electrolyzers is obtained using the equation below:

$$V_{cell} = V_{rev} + V_{act} + V_{ohm} \quad (13)$$

$$V_{act} = s \log \left( \frac{t_1 + \frac{t_2}{T} + \frac{t_3}{T^2}}{A} I + 1 \right) \quad (14)$$

$$V_{ohm} = \frac{r_1 + r_2 T}{A} I \quad (15)$$

where  $V_{act}$  and  $V_{ohm}$  are the activation and ohmic voltages that are in relation with the activation losses and ohmic losses of the cell, respectively. The  $I$  and  $A$  parameters are the electrical current applied to the cell and the electrode area (=0.25 m<sup>2</sup> in this work), respectively. The Faraday efficiency is obtained using the following equation:

$$\eta_F = \frac{\left( \frac{I}{A} \right)^2 f_2}{f_1 + \left( \frac{I}{A} \right)^2 f_2} \quad (16)$$

and the total hydrogen and oxygen produced by the proposed electrolyzer can be defined as:

$$\dot{n}_{H_2} = 2\dot{n}_{O_2} = \eta_F \frac{n_c I}{zF} \quad (17)$$

The  $n_c$  parameter in the above equation is the number of cells in the electrolyzer, which equals to 21 cells in this work. In order to calculate the heat transfer between the electrolyzer and ambient, the quasi-state thermal model is provided as:

$$T = T_i + \frac{\Delta t}{C_t} (\dot{Q}_{gen} - \dot{Q}_{loss} - \dot{Q}_{cool}) \quad (18)$$

$$\dot{Q}_{gen} = \eta_c (V_{cell} - V_{tn}) \quad (19)$$

$$\dot{Q}_{loss} = \frac{1}{R_t} (T - T_a) \quad (20)$$

$$\dot{Q}_{cool} = C_{cw} (T_{cw,i} - T_{cw,o}) \quad (21)$$

where  $T$ ,  $T_i$ ,  $\Delta t$ ,  $C_t$ ,  $\dot{Q}_{gen}$ ,  $\dot{Q}_{loss}$ , and  $\dot{Q}_{cool}$  are the cell temperature, initial cell temperature, time interval, overall thermal capacity of the electrolyzer, total heat generated in the electrolyzer, total heat loss to the environment,

and total heat transferred to the cooling water, respectively. The overall thermal resistance was calculated by defining the cooling pattern for the electrolyzer for a number of different days [41]:  $C_t = 625 \text{ kJ } ^\circ\text{C}^{-1}$  and  $R_t = 0:167 \text{ } ^\circ\text{C W}^{-1}$  (equal to  $\tau_t = 29 \text{ h}$ ). The equation used for determination of time constant ( $\tau_t$ ) can be expressed as [41]:

$$\tau_t = C_t R_t \tag{22}$$

Furthermore, the constant parameters used in the mentioned equations are provided in Table 2 [41, 42].

**Table 2. Constant parameters used in the alkaline electrolyzer model [41, 42].**

Parameter	Unit	Value
$r_1$	$\Omega \text{ m}^2$	8.05e-5
$r_2$	$\Omega \text{ m}^2/^\circ\text{C}$	-2.5e-7
$s$	V	0.185
$t_1$	$\text{A m}^2$	1.002
$t_2$	$\text{m}^2 \text{ } ^\circ\text{C}/\text{A}$	8.424
$t_3$	$\text{m}^2 \text{ } ^\circ\text{C}^2/\text{A}$	247.3

In order to calculate the  $f_1$  and  $f_2$  parameters, the values of which depend on temperature, the following equations are utilized [41, 42]:

$$f_1 = 50 + 2.5T + (5.082E - 19)T^2 \tag{23}$$

$$f_2 = 1 - (2.5E - 4)T - (5.346E - 21)T^2 \tag{24}$$

#### 4. Validation

In order to validate the AEL model presented in the last section, the results obtained were compared with the references [41, 42]. The comparison of cell voltage and faraday efficiency for different cell temperatures in various current densities in the proposed model and reference are presented in Figures 2 and 3, respectively. As it could be seen in these figures, the same results were obtained in the proposed AEL model, compared to the reference values, which confirmed that the model was reliable.

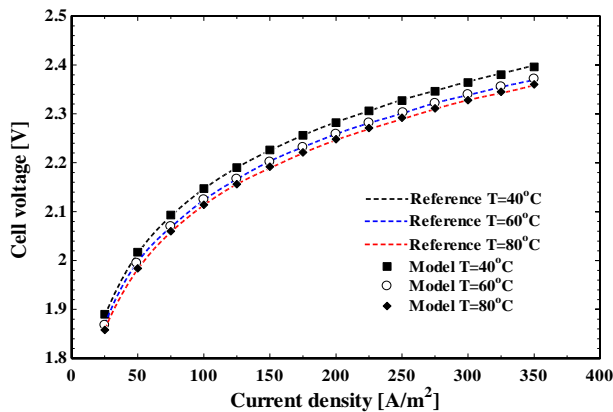


**Figure 2. Cell voltage for different cell temperatures in various current densities in the proposed model and references [41, 42].**

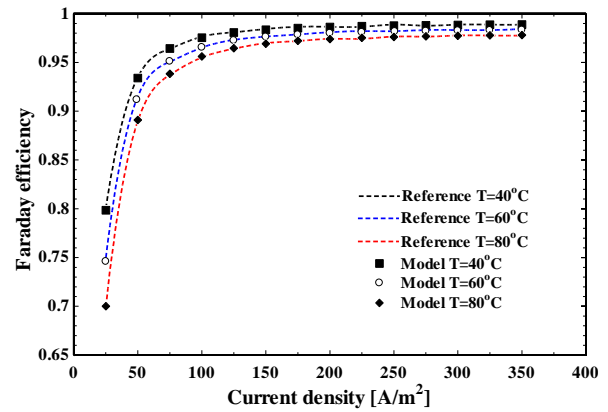


**Figure 3. Faraday efficiency for different cell temperatures in various current densities in the proposed model and reference.**

#### 5. Result and Discussion

The climate conditions of the city of Shahrood were considered as the input parameters of the model. The variation in the average temperature of this city is provided in Figure 4. Furthermore, the geographic latitude of this city (being equal to  $36.4^\circ$ ) was used as the input of the model for calculation of the solar irradiation. The total area of the installed PV panels was considered to be  $50 \text{ m}^2$  in this work. The dates employed as the indicators of the weathers of the spring, summer, fall, and winter seasons based on the Iranian climate are presented in Table 3.

**Table 3. Dates that are indicators of various season climates in Iran [36].**

Season	Date
Spring	20 <sup>th</sup> of March
Summer	21 <sup>st</sup> of June
Fall	22 <sup>nd</sup> of September
Winter	21 <sup>st</sup> of December

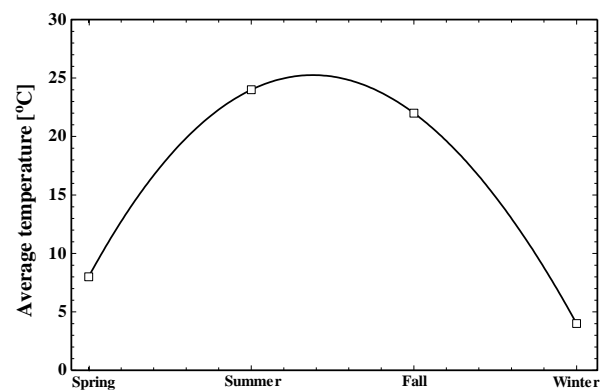


**Figure 4. Average ambient temperature of the city of Shahrood in various seasons.**

Figure 5 shows the percentage of the extra power absorbed by the PV panels using the single-axis solar tracker in different seasons. As it could be seen, the PV panel power generation rate increased by approximately 0.25%, 17%, 0.65%,

and 2.3% in the spring, summer, fall, and winter, respectively. The rate of electrical power generated by the PV panels in different hours of the day during the year is presented in Figure 6. Based on the results presented in this figure, the maximum peak power produced by PVs in the summer equals to 4.2 kW. Furthermore, the minimum and maximum hours of sunlight belong to the winter and summer, respectively, as it can be seen in this figure.

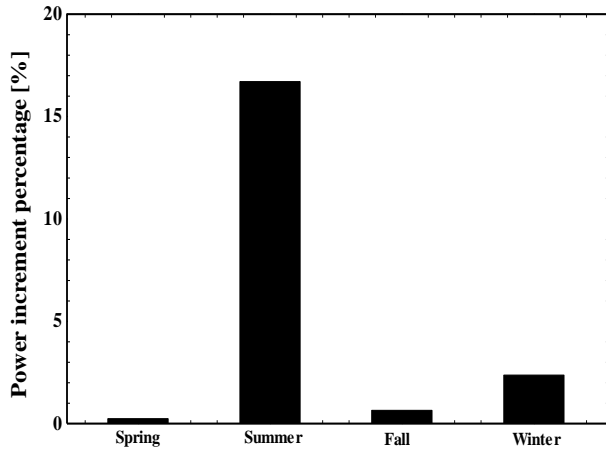


Figure 5. Solar power absorption increment percentage in various seasons by employment of a single-axis solar tracker.

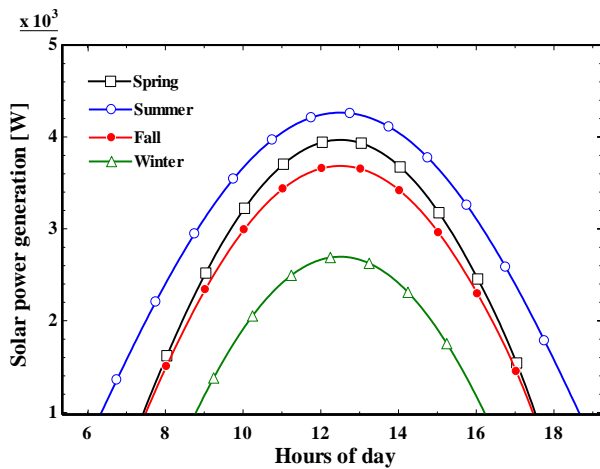


Figure 6. SOLAR POWER GENERATED BY THE PV PANELS IN DIFFERENT HOURS OF THE DAY IN VARIOUS SEASONS.

The variation in the efficiency of the PV panels in different hours of the day is shown in Figure 7. As it could be clearly seen in this figure, the maximum efficiency of the PV panels was achieved in the winter, which was between 12.5% and 13%, while the efficiency of the PV panels in the spring was around 12.25%. Moreover, the PV panel efficiency in the summer and fall was predicted to be between 10.75% and 12% in different hours of the day. While the efficiency of PV in the summer was the lowest due to increment of its cell temperature, the proportion of the solar energy absorbed in the summer was still

more than the other seasons, resulting in more power production by the PV panels in the summer compared to the other seasons (see Figure 6).

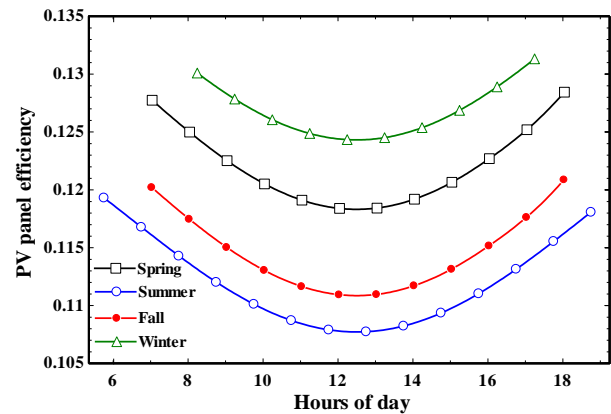


Figure 7. PV PANEL EFFICIENCY IN VARIOUS HOURS OF THE DAY IN DIFFERENT SEASONS.

The PV panel output electrical current in various hours of the day is shown in Figure 8 for different seasons. In fact, the electrical current at the output of the DC-DC converter was used in this figure. As it could be seen, the maximum electrical current peak reached 80 A in the summer, and then it decreased to approximately 74 A and 68 A in the spring and fall, respectively. In addition, it decreased up to 50 A in the winter. The variation in the electrical current input of the electrolyzer affects its cell operating temperature, as it can be seen in Figure 9. As the maximum peak current was reached in the summer, the maximum temperature of the electrolyzer operating temperature cell is achieved in this season, which equals to almost 80 °C. The peak cell temperature in the fall is higher than that in the spring because the ambient temperature in the fall is higher than spring, resulting in achieving a higher initial cell temperature in the fall.

The range of hourly ohmic voltage changes for each electrolyzer cell in various seasons is indicated in Figure 10. The increment of ohmic resistance of the cell results in an increase in its temperature, leading to the generation of more waste heat and reduction of faraday efficiency. The ohmic voltage is also called the ohmic over-voltage of the cell. As it can be seen in Figure 10, the ohmic voltage of each cell in the summer and spring reaches its maximum amount, which equals to 0.021V, and its peak decreased to 0.019 and 0.015 in the fall and winter, respectively.

Figure 11 presents the hydroxy gas production rate of the system and the electrolyzer average Faraday efficiency for various seasons of the year. The rate of hydroxy production rate is 7.6 m<sup>3</sup>/day, 9.4 m<sup>3</sup>/day, 10.4 m<sup>3</sup>/day, and 4.1 m<sup>3</sup>/day in the spring, summer, fall, and winter in the city of

Shahrood, respectively. Furthermore, the maximum average Faraday efficiency of the cells is achieved in the summer, while the minimum average Faraday efficiency is achieved in the winter because of the lower electrical current produced by the PV panels in the winter compared to the summer.

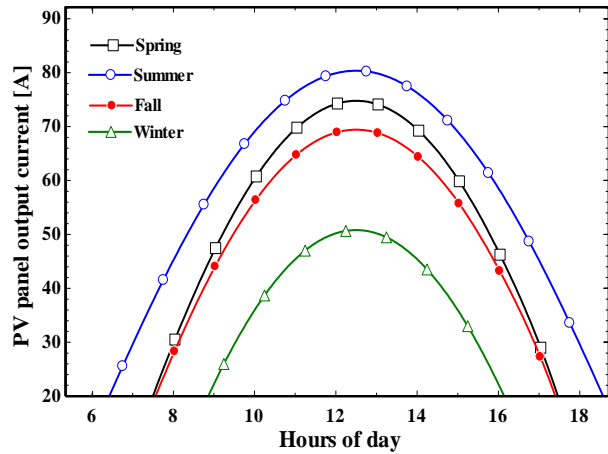


Figure 8. PV panel output electrical current in various hours of the day in different seasons.

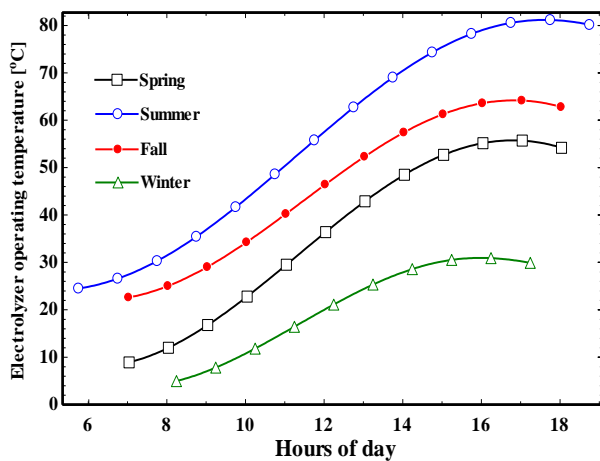


Figure 9. Electrolyzer stack operating temperature in various hours of the day in different seasons.

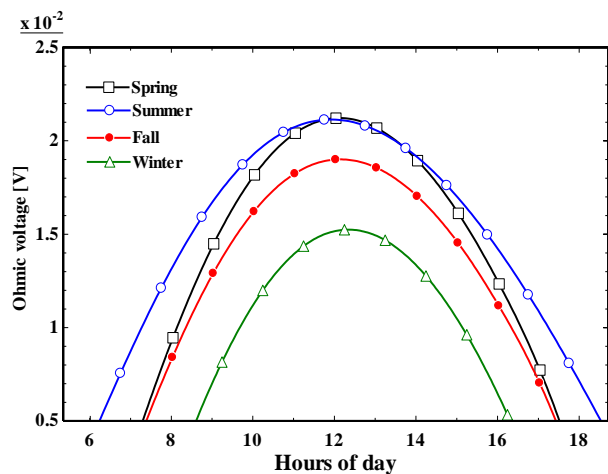


Figure 10. Ohmic voltage of each electrolyzer cell in various hours of the day in different seasons.

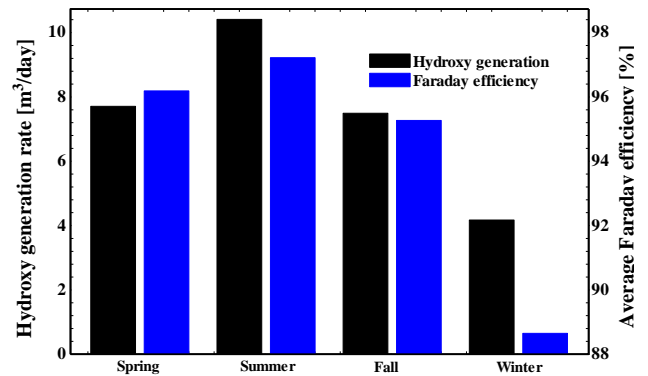


Figure 11. Hydroxy gas generation rate and average Faraday efficiency of the electrolyzer in various seasons of the year.

### 5. Conclusions

The hydroxy gas is one of the green fuels that can be used in the transportation systems as an alternative to the fossil fuels. In this work, the thermodynamic analysis of an alkaline electrolyzer producer of hydroxy gas integrated with photovoltaic panels equipped with a single-axis solar tracking system was performed. In order to simulate the integrated systems, the transient mathematical model of the alkaline electrolyzer and PV panels was developed and written in the EES software. The main aim of this work was to provide a transient analysis of a stand-alone hydroxy production system for investigation of the variations in the system functional parameters in various conditions during the year. It was assumed that the proposed solar driven hydroxy generation system was installed in the city of Shahrood, and the climate data of this city was used in the simulations. Then the hourly changes of the electrolyzer parameters in various seasons during the year were analyzed. The main conclusions drawn from this work can be listed as follow:

- By installation of the PV panels with an area of 50 m<sup>2</sup>, up to 4.2 kW electrical power could be generated. In addition, the electrical current peak generated by PVs was between 50 A and 80 A in various seasons during the year.
- The proposed alkaline electrolyzer operating temperature reached 80 °C in the summer; however, its peak temperatures were 66 °C, 56 °C, and 32 °C in the fall, spring, and winter, respectively.
- The peak ohmic voltage of the electrolyzer cells reached 0.021 V in the spring and summer, and then its peak decreased to 0.019V and 0.015V in the fall and winter, respectively.
- The rate of the hydroxy gas generation was 7.6 m<sup>3</sup>/day in the spring. It increased to 10.4

m<sup>3</sup>/day in the summer, which was the maximum hydroxy generation rate of the proposed electrolyzer. After that, it decreased to 7.2 m<sup>3</sup>/day and 4.1 m<sup>3</sup>/day in the fall and winter, respectively.

## 6. Appendix

### a. Nomenclature

$I$	Solar irradiation [J/m <sup>2</sup> ]
$\omega$	Solar hour angle [degree]
$\theta$	Angle of incident [degree]
$\beta$	Tilt angle [degree]
$\phi$	Geographic latitude [degree]
$\delta$	Declination angle [degree]
$\gamma$	Azimuth angle [degree]
$V$	Cell voltage [V]
$G$	Gibbs free energy
$z$	Number of electrons
$F$	Faraday constant
$T$	Cell operating temperature [°C]
$I$	Electrical current [A]
$A$	Electrode area [m <sup>2</sup> ]
$\dot{n}$	Molar flow rate [mol/s]
$\dot{W}$	Electrical power [W]
$\Delta t$	Time interval [s]
$\dot{Q}$	Heat Transfer rate [W]

### b. Subscripts

$sc$	Solar constant
$T$	Tracker
$b$	Beam
$d$	Diffuse
$amb$	Ambient
$rev$	Reversible
$act$	Activation
$ohm$	Ohmic
$i$	Initial

## 7. References

[1] Naseri A, Fazlikhani M, Sadeghzadeh M, Naeimi A, Bidi M, and Tabatabaei SH. Thermodynamic and Exergy Analyses of a Novel Solar-Powered CO<sub>2</sub> Transcritical Power Cycle with Recovery of Cryogenic LNG using Stirling Engines. *Renewable Energy Research and Application*. 2020;1(2):175-85.

[2] Alayi R and Jahanbin F. Generation Management Analysis of a Stand-alone Photovoltaic System with Battery. *Renewable Energy Research and Application*. 2020;1(2):205-9.

[3] Salek F, Zamen M, and Hosseini SV. Experimental study, energy assessment, and improvement of hydroxy generator coupled with a gasoline engine. *Energy Reports*. 2020;6:146-56.

[4] Thanompongchart P and Tippayawong N. Experimental investigation of biogas reforming in gliding arc plasma reactors. *International Journal of Chemical Engineering*. 2014;2014.

[5] Salek F, Zamen M, Hosseini SV, and Babaie M. Novel hybrid system of pulsed HHO generator/TEG waste heat recovery for CO reduction of a gasoline engine. *International Journal of Hydrogen Energy*. 2020;45(43):23576-86.

[6] Zhao H, Nie T, Zhao H, Liu Y, Zhang J, Ye Q *et al*. Enhancement of Fe-C Micro-electrolysis in Water by Magnetic Field: Mechanism, Influential Factors and Application Effectiveness. *Journal of Hazardous Materials*. 2020:124643.

[7] Bos M, Kersten S, and Brilman D. Wind power to methanol: Renewable methanol production using electricity, electrolysis of water and CO<sub>2</sub> air capture. *Applied Energy*. 2020;264:114672.

[8] Fang H, Haibin L, and Zengli Z. Advancements in development of chemical-looping combustion: a review. *International Journal of Chemical Engineering*. 2009;2009.

[9] Ghorbani B, Mehrpooya M, and Sadeghzadeh M. Process development of a solar-assisted multi-production plant: Power, cooling, and hydrogen. *International Journal of Hydrogen Energy*. 2020;45(55):30056-79.

[10] Riyadi BS. Culture of Abuse of Power due to Conflict of Interest to Corruption for Too Long on the Management form Resources of Oil and Gas in Indonesia. *International Journal of Criminology and Sociology*. 2020;9:247-54.

[11] Woollacott J. A bridge too far? The role of natural gas electricity generation in the US climate policy. *Energy Policy*. 2020;147:111867.

[12] Ahmadi A, Jamali D, Ehyaei M, and Assad MEH. Energy, exergy, economic, and exergoenvironmental analyses of gas and air bottoming cycles for production of electricity and hydrogen with gas reformer. *Journal of Cleaner Production*. 2020;259:120915.

[13] Ahmadi MH, Ghazvini M, Sadeghzadeh M, Alhuyi Nazari M, Kumar R, Naeimi A *et al*. Solar power technology for electricity generation: A critical review. *Energy Science & Engineering*. 2018;6(5):340-61.

[14] Ahmadi MH, Banihashem SA, Ghazvini M, and Sadeghzadeh M. Thermo-economic and exergy assessment and optimization of performance of a hydrogen production system by using geothermal energy. *Energy and Environment*. 2018;29(8):1373-92.

- [15] Rashid MM, Al Mesfer MK, Naseem H, and Danish M. Hydrogen production by water electrolysis: a review of alkaline water electrolysis, PEM water electrolysis and high temperature water electrolysis. *Int J Eng Adv Technol*. 2015;4(3):2249-8958.
- [16] Ezzahra Chakik F, Kaddami M, and Mikou M. Effects of operating parameters on hydrogen production by electrolysis of water. *international journal of hydrogen energy*. 2017;42(40):25550-7.
- [17] Ghazvini M, Sadeghzadeh M, Ahmadi MH, Moosavi S, and Pourfayaz F. Geothermal energy use in hydrogen production: A review. *International Journal of Energy Research*. 2019;43(14):7823-51.
- [18] Khosravi A, Rodriguez ORS, Talebjedi B, Laukkanen T, Pabon JJG, and Assad MEH. New Correlations for Determination of Optimum Slope Angle of Solar Collectors. 2020.
- [19] Menad CA, Gomri R, and Bouchahdane M. Data on safe hydrogen production from the solar photovoltaic solar panel through alkaline electrolyser under Algerian climate. *Data in brief*. 2018;21:1051-60.
- [20] M. Sultan S, Tso CP, M. NEE. A Case Study on Effect of Inclination Angle on Performance of Photovoltaic Solar Thermal Collector in Forced Fluid Mode. *Renewable Energy Research and Application*. 2020;1(2):187-96.
- [21] Touili S, Merrouni AA, El Hassouani Y, Amrani A-i, and Rachidi S. Analysis of the yield and production cost of large-scale electrolytic hydrogen from different solar technologies and under several Moroccan climate zones. *International Journal of Hydrogen Energy*. 2020;45(51):26785-99.
- [22] Beigzadeh M, Pourfayaz F, and Pourkiaei S. Modeling Heat and Power Generation for Green Buildings based on Solid Oxide Fuel Cells and Renewable Fuels (Biogas). *Renewable Energy Research and Application*. 2020;1(1):55-63.
- [23] Castrillo EDR, Santaella JRB, Assad MEH, Khosravi A, and Pabón JJG, editors. Modeling and validation of a commercial dry electrolytic cell for the production of oxyhydrogen. 2020 *Advances in Science and Engineering Technology International Conferences (ASET): IEEE*.
- [24] Ruuskanen V, Koponen J, Huoman K, Kosonen A, Niemelä M, and Ahola J. PEM water electrolyzer model for a power-hardware-in-loop simulator. *International Journal of Hydrogen Energy*. 2017;42(16):10775-84.
- [25] Guo Y, Li G, Zhou J, and Liu Y, editors. Comparison between hydrogen production by alkaline water electrolysis and hydrogen production by PEM electrolysis. *IOP Conference Series: Earth and Environmental Science*; 2019: IOP Publishing.
- [26] Keçebaş A, Kayfeci M, and Bayat M. Electrochemical hydrogen generation. *Solar Hydrogen Production: Elsevier*; 2019. p. 299-317.
- [27] Navarro R, Guil R, and Fierro J. Introduction to hydrogen production. *Compendium of Hydrogen Energy: Elsevier*; 2015. p. 21-61.
- [28] Dehghanimadvar M, Shirmohammadi R, Sadeghzadeh M, Aslani A, and Ghasempour R. Hydrogen production technologies: Attractiveness and future perspective. *International Journal of Energy Research*.
- [29] Fereidooni M, Mostafaeipour A, Kalantar V, and Goudarzi H. A comprehensive evaluation of hydrogen production from photovoltaic power station. *Renewable and Sustainable Energy Reviews*. 2018;82:415-23.
- [30] Schnuelle C, Wassermann T, Fuhrlaender D, and Zondervan E. Dynamic hydrogen production from PV and wind direct electricity supply—Modeling and techno-economic assessment. *International Journal of Hydrogen Energy*. 2020;45(55):29938-52.
- [31] Bhattacharyya R, Misra A, and Sandeep K. Photovoltaic solar energy conversion for hydrogen production by alkaline water electrolysis: conceptual design and analysis. *Energy Conversion and management*. 2017;133:1-13.
- [32] Ferrari M, Rivarolo M, and Massardo A. Hydrogen production system from photovoltaic panels: experimental characterization and size optimization. *Energy Conversion and Management*. 2016;116:194-202.
- [33] Cilogulları M, Erden M, Karakilcik M, and Dincer I. Investigation of hydrogen production performance of a Photovoltaic and Thermal System. *international journal of hydrogen energy*. 2017;42(4):2547-52.
- [34] Maatallah T, El Alimi S, and Nassrallah SB. Performance modeling and investigation of fixed, single and dual-axis tracking photovoltaic panel in Monastir city, Tunisia. *Renewable and Sustainable Energy Reviews*. 2011;15(8):4053-66.
- [35] Afanasyeva S, Bogdanov D, and Breyer C. Relevance of PV with single-axis tracking for energy scenarios. *Solar Energy*. 2018;173:173-91.
- [36] Duffie JA, Beckman WA, and Blair N. *Solar engineering of thermal processes, photovoltaics and wind*: John Wiley & Sons; 2020.
- [37] Zhang D and Allagui A. Fundamentals and performance of solar photovoltaic systems. *Design and Performance Optimization of Renewable Energy Systems: Elsevier*; 2021. p. 117-29.
- [38] Pourderogar H, Harasii H, Alayi R, Delbari SH, Sadeghzadeh M, and Javaherbakhsh AR. Modeling and Technical Analysis of Solar Tracking System to Find Optimal Angle for Maximum Power Generation using

MOPSO Algorithm. *Renewable Energy Research and Application*. 2020;1(2):211-22.

[39] Olukan TA and Emziane M. A comparative analysis of PV module temperature models. *Energy Procedia*. 2014;62(2):694-703.

[40] Fesharaki VJ, Dehghani M, Fesharaki JJ, and Tavasoli H, editors. Effect of temperature on photovoltaic cell efficiency. *Proceedings of the 1st International Conference on Emerging Trends in Energy Conservation–ETEC*, Tehran, Iran; 2011.

[41] Ulleberg Ø. Modeling of advanced alkaline electrolyzers: a system simulation approach. *International journal of hydrogen energy*. 2003;28(1):21-33.

[42] Tijani AS, Yusup NAB, Rahim AA. Mathematical modelling and simulation analysis of advanced alkaline electrolyzer system for hydrogen production. *Procedia Technology*. 2014;15:798-806.